Analytic description of monodromy oscillons

D. G. Levkov[1,2,*] and V. E. Maslov[1,2,3,†]

[1]*Institute for Nuclear Research of the Russian Academy of Sciences, Moscow 117312, Russia*
[2]*Institute for Theoretical and Mathematical Physics, MSU, Moscow 119991, Russia*
[3]*Department of Particle Physics and Cosmology, Faculty of Physics, MSU, Moscow 119991, Russia*

(Received 13 June 2023; accepted 18 August 2023; published 15 September 2023)

We develop a precise analytic description of oscillons—long-lived quasiperiodic field lumps—in scalar field theories with nearly quadratic potentials, e.g., the monodromy potential. Such oscillons are essentially nonperturbative due to large amplitudes, and they achieve extreme longevities. Our method is based on a consistent expansion in the anharmonicity of the potential at strong fields, which is made accurate by introducing a field-dependent "running mass." At every order, we compute effective action for the oscillon profile and other parameters. Comparison with explicit numerical simulations in $(3+1)$-dimensional monodromy model shows that our method is significantly more precise than other analytic approaches.

DOI: 10.1103/PhysRevD.108.063514

I. INTRODUCTION

Oscillons [1–4] are long-lived pulsating field configurations that emerge in many classical theories, specifically, in models of a scalar field $\varphi(t,\boldsymbol{x})$ [5–11]. With time, these objects demise by emitting radiation. Nevertheless, their existence may affect a wide range of cosmological phenomena [12–15], from inflationary preheating [16–19] to phase transitions [20–22] and generation of axion dark matter [4,23,24].

In some models oscillons live exceptionally long [9,25,26]. An important example is a scalar field theory with the monodromy potential [16,25,27]

$$V(\varphi) = \frac{1}{2p}(1+\varphi^2)^p, \quad p \lesssim 1, \tag{1}$$

see Fig. 1. Hereafter we use dimensionless units[1] with particle mass $m = 1$.

Oscillons in the model (1) exist and last for up to 10^{14} periods [9]. Their lifetimes are considerably larger at $p \approx 1$ when the potential is almost quadratic. This last property is generic: oscillons with extreme longevities are expected to appear in models with suppressed interactions [9,28].

[*]levkov@ms2.inr.ac.ru
[†]vasilevgmaslov@ms2.inr.ac.ru
[1]Physical dimensions can be restored by rescaling $\varphi \to \varphi/F$, $t \to mt$, and $\boldsymbol{x} \to m\boldsymbol{x}$, which gives $V = m^2F^2(1+\varphi^2/F^2)^p/2p$.

Monodromy oscillons significantly alter some cosmological scenarios described by the model (1). They may form and produce gravitational waves [16,27,29] at the reheating stage of the monodromy inflation [30–32] where φ represents inflaton and $p = 1/2$. At $p \approx 1$ long-lived monodromy oscillons may impact cosmological evolution and even form a (part of) scalar field dark matter [9,25].

The aim of this paper is to develop a consistent, practical, and precise analytic approach to oscillons in theories with nearly quadratic potentials. It would be logical to organize such a technique as an asymptotic expansion in the inverse oscillon lifetime $\tau^{-1} \ll m$. However, the parameter τ is not built into the field theory Lagrangian and cannot be used directly. That is why all practical descriptions of oscillons use other—convenient—expansion parameters.

Presently, there are two[2] general analytic approaches to oscillons, and both are useless in the model (1). The first hope is a perturbative expansion [35–39], since weakness of interactions may suppress wave emission and guarantee longevity. For the potential (1), this is equivalent to expansion in small field amplitudes $|\varphi| \ll 1$ which—alas—does not work inside the oscillons because their fields are strong, $\varphi \sim \varphi_0 \gg 1$. We demonstrate this in Fig. 1 by comparing at $|\varphi| \gg 1$ the potential with its quadratic part $m^2\varphi^2/2$ (solid and dotted lines).

The second "Effective Field Theory" (EFT) approach [28] is based on the observation [40] that spatial sizes of the longest-living oscillons are large, $R \gg m^{-1}$. This is true, in particular, for oscillons in the model (1). It is natural to expect that such large objects evolve slowly at time scales

[2]Some other witty tricks [33,34] have limited region of validity and also do not apply in the model (1).

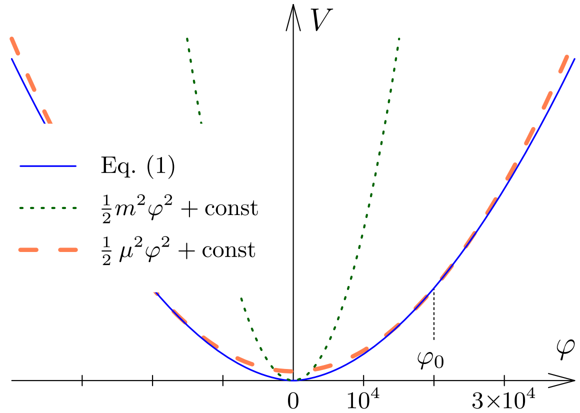

FIG. 1. The potential (1) (solid line) approximated by the leading term of its perturbative expansion around the vacuum (dotted) and the first term in Eq. (2) (dashed). Typical field inside oscillons is indicated by $\varphi \sim \varphi_0$. Here we use $p = 0.9$ and $\varphi_0 = 2 \times 10^4$.

$t \sim R$ considerably exceeding their oscillation periods $T \sim m^{-1}$. Then their stability can be related to the conservation of adiabatic invariant N [41,42]. Nevertheless, direct asymptotic expansion in R^{-1} [28] is of a limited practical use because it exploits general nonlinear spatially homogeneous solutions which cannot be obtained analytically in the model (1).

In this paper we merge the above two approaches together into a general, simple and precise analytic technique applicable in the model (1). On the one hand, we remedy the perturbative method by noting that the potential (1) with p somewhat below 1 can be approximated by a parabola $\mu^2\varphi^2/2$ in every vast region $\varphi \sim O(\varphi_0)$, where φ_0 is arbitrarily large. The latter parabolas, however, essentially differ from the leading Taylor term of the potential near the vacuum, as their curvatures μ^2 change with φ_0—cf. the dashed, solid, and dotted lines in Fig. 1. This means that the scalar particles interact weakly even in the strong-field regions, but their "mass" μ slowly depends on φ. We therefore write

$$V(\varphi) = \mu^2\varphi^2/2 + \delta V(\varphi), \qquad \delta V \equiv V(\varphi) - \mu^2\varphi^2/2, \quad (2)$$

where $\mu \neq m$, and perform expansion[3] in δV. Since Eq. (2) is a trivial identity, the result does not depend on μ which is made field-dependent in the end of the calculation. We will see that this trick with field-dependent μ radically increases precision, working in a similar way to scale-dependent renormalized constants in quantum field theory (QFT). On the other hand, weak interactions imply large sizes of bound states—oscillons—so we perform further expansion in the inverse oscillon radius R^{-1}. The accuracy of the overall method does not deteriorate even at extremely large oscillon amplitudes, although this technique is less effective for essentially nonlinear potentials with small p.

To sum up, our expansion parameters are $(\partial_i\varphi)^2 \ll \mu^2\varphi^2$ and $\delta V \ll \mu^2\varphi^2$. At every order, we analytically obtain effective action for the oscillon profiles, find expressions for their adiabatic charges N and energies E. At the roughest level, our method is close to the single-frequency approximation, a popular and practical heuristic technique [11,26,43,44]. We provide a recipe for computing corrections thus upgrading this technique to a consistent asymptotic expansion.

The paper is organized as follows. We start in Sec. II by illustrating the new method in a toy mechanical model. Then we apply it to field-theoretical oscillons in Sec. III and confirm its predictions with exact numerical simulations in Sec. IV. Corrections are considered in Sec. V. Section VI contains discussion and comparison to other analytic approaches.

II. TOY MODEL: A MECHANICAL OSCILLATOR

For a start, let us illustrate the key trick of this paper in the mechanical model of nonlinear oscillator with the potential (1). Its coordinate $\varphi = \varphi(t)$ satisfies the equation

$$\partial_t^2\varphi = -V'(\varphi) \equiv -\varphi(1+\varphi^2)^{-\varepsilon}, \qquad \varepsilon \equiv 1 - p, \quad (3)$$

which is not exactly solvable; here the prime denotes φ derivative.

At $\varepsilon \ll 1$ and $p \approx 1$, however, the nonlinearities are small, so we can approximately integrate the equation as follows. We add the auxiliary quadratic term $\mu^2\varphi^2/2$ to the potential and subtract it back,

$$\partial_t^2\varphi = -\mu^2\varphi - \delta V'(\varphi), \qquad \delta V \equiv V - \mu^2\varphi^2/2, \quad (4)$$

cf. Eq. (2). The nonlinear force $\delta V'$ is weak if μ^2 is close to the curvature of the potential. We achieve this by choosing

$$\mu^2 = V'(\varphi_0)/\varphi_0 \equiv (1+\varphi_0^2)^{-\varepsilon}, \quad (5)$$

where the "renormalization scale" φ_0 will be tuned soon to the typical oscillator amplitude. The proper choice (5) allows us to develop a consistent expansion in small δV.

To the zeroth order in the last term, Eq. (4) describes linear oscillations with frequency μ. It can be solved by performing a canonical transformation from the coordinate φ and momentum $\pi_\varphi \equiv \partial_t\varphi$ to the action-angle variables,

$$\varphi = \sqrt{2I/\mu}\cos\theta, \qquad \pi_\varphi = -\sqrt{2I\mu}\sin\theta. \quad (6)$$

Here $I(t)$ and $\theta(t)$ characterize the amplitude and phase of the oscillations, respectively. Namely, the evolution without the δV term would be $I = \text{const}$ and $\theta = \mu t$.

[3]In Eq. (2) we ignore the constant part of the potential which does not affect the field equation.

The next step is to include nonlinear corrections in δV. It is convenient to do that on the level of classical action,

$$\mathcal{S} = \int dt[\pi_\varphi \partial_t \varphi - H] = \int dt[I\partial_t \theta - H(I,\theta)], \quad (7)$$

where the Hamiltonian is

$$H = \frac{1}{2}\pi_\varphi^2 + V(\varphi) = \mu I + \delta V(I,\theta), \quad (8)$$

and we performed the transformation (6) in the second equalities.

It is worth stressing that I and θ are not the true action-angle variables of the full nonlinear oscillator. Hence, the perturbation δV may cause I and $\partial_t\theta$ to drift slowly, and also equips them with tiny oscillating corrections. Below we consider stationary solutions on long timescales. In this case the integral (7) averages the perturbations over many periods. Since θ evolves linearly in the zeroth-order approximation, we can perform the averaging by integrating[4] over it,

$$\delta V \to \langle \delta V \rangle = \int_0^{2\pi} \frac{d\theta}{2\pi} \delta V(\theta) = \frac{1}{2p}(\mathcal{A}_p(\varsigma) - p\mu I), \quad (9)$$

where $\varsigma = 2I/\mu$,

$$\begin{aligned}\mathcal{A}_p(\varsigma) &\equiv \langle (1+\varsigma\cos^2\theta)^p \rangle \\ &= (1+\varsigma)^{p/2} P_p\left(\frac{1+\varsigma/2}{\sqrt{1+\varsigma}}\right),\end{aligned} \quad (10)$$

and $P_p(x) \equiv {}_2F_1[-p, p+1; 1; (1-x)/2]$ is the Legendre function.

Together, Eqs. (7), (8), and (9) form an effective action describing long-term behavior of the monodromy oscillator. We obtained it to the leading order in δV.

Now, we make a crucial step: choose the parameter μ and its arbitrary "scale" φ_0 in Eq. (5). The approximate action (7), (8), (9) depends on φ_0, but very weakly: its variation with respect to that parameter is $O(\delta V^2) \sim O(\varepsilon^2)$. Indeed, μ cancels itself in the exact action (7) and resurfaces in the approximate results only because we ignored μ-dependent corrections. If we continued computations to the n-th order in δV, the sensitivity of the effective action to φ_0 and μ would be $O(\varepsilon^{n+1})$. Thus, we are free to choose φ_0 in any reasonable way that decreases δV and increases the precision of the expansion. Specifically, we adjust φ_0 to the field amplitude[5] in Eq. (6),

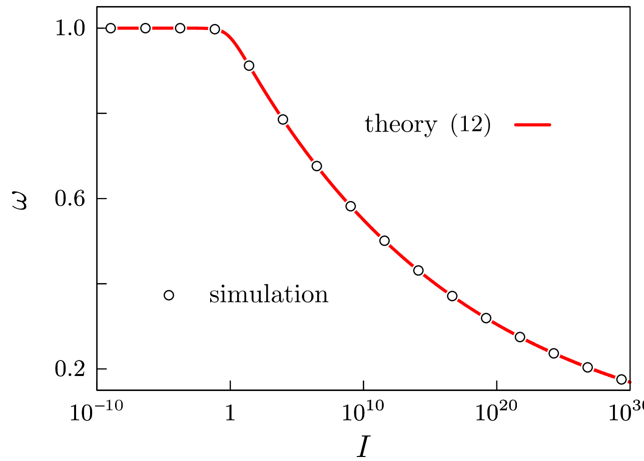

FIG. 2. Frequency ω of the monodromy oscillator as a function of the action variable I; we use $p = 0.95$. Solid line and circles show the theory (12) and exact numerical results, respectively.

$$\varphi_0 = \sqrt{2I}. \quad (11)$$

This makes $\mu = \mu(I)$ depend on the action variable.

Equations for the long-term motions of the monodromy oscillator are obtained by varying the effective action (7), (8), (9) with respect to $I(t)$ and $\theta(t)$. We get $\theta = \omega t$ and

$$\omega = \mu + (\partial_\varsigma \mathcal{A}_p/\mu^2 p - 1/2)(\mu - I\partial_I \mu), \quad (12)$$

where $\varsigma = 2I/\mu$ and $\partial_I\mu = -\varepsilon(1+2I)^{-\varepsilon/2-1}$. Equation (12) gives oscillation frequency $\omega = \omega(I)$ as a function of the action variable.

To test the method, we compare Eq. (12) with the exact frequency $\omega(I)$ of the monodromy oscillator at $p = 0.95$; see Fig. 2. The latter is computed by numerically evolving Eq. (3) and then extracting the oscillation period $T = 2\pi/\omega$ and the action variable $I = \oint \pi_\varphi d\varphi/2\pi$. Figure 2 shows that the theory has a remarkable relative precision $\Delta\omega/\omega \sim 10^{-4}$ which remains stable even in the case of exceptionally large amplitudes $I \sim 10^{30}$.

The secret of high accuracy is hidden in two tricks. First, we correctly selected the values of artificial parameters φ_0 and $\mu(\varphi_0)$, and even allowed them to "run"—depend on I—in the end. This approach is similar to running of the renormalized constants in QFT. Second, despite working at small $\varepsilon \equiv 1 - p$, we did *not* directly expand δV in this parameter: The latter expansion actually goes in $\varepsilon \ln|\varphi|$ and breaks at large amplitudes $|\varphi| \gtrsim e^{1/2\varepsilon}$.

It is worth noting that corrections to the effective action (7), (8), (9) can be computed in a straightforward manner, by taking higher-order δV contributions into account. We will work them out in Sec. V when effective action in field theory is introduced.

[4]This and other θ averages can be recast as contour integrals $\langle f \rangle = \oint f(z)dz/(2\pi i z)$ over the unit circle $z = e^{2i\theta}$, $|z| = 1$.

[5]Alternatively, one can find $\varphi_0(I)$ from the equation $\varphi_0^2 = 2I/\mu$, where μ is still given by Eq. (5). This method gives slightly better results at extremely large amplitudes when μ is significantly smaller than 1.

III. EFFECTIVE FIELD THEORY FOR OSCILLONS

Let us turn to oscillons—long-lived solutions of the field equation

$$\partial_t^2\varphi - \Delta\varphi = -V'(\varphi) \tag{13}$$

with the monodromy potential (1). For definiteness, we will work in $3+1$ dimensions: Generalizations to other cases are straightforward. We perform the trick (2): extract the quadratic part of the potential $\mu^2\varphi^2/2$ and then work order-by-order in the remaining part δV. Now, the equation includes a spatial derivative $\Delta\varphi$ which also can be treated perturbatively. Indeed, $\Delta\varphi$ and $\delta V'$ are comparable inside the oscillons because these objects are held by weak attractive self-force compensating repulsive contributions of the derivatives ("quantum pressure"). As a consequence, the oscillon sizes are parametrically large: $R^{-2} \sim O(\delta V) \sim O(\varepsilon)$.

To the zeroth order in δV, we have the same linear oscillator $\partial_t^2\varphi = -\mu^2\varphi$ as in the previous section, where $\mu(\varphi_0)$ again estimates local curvature of the potential via Eq. (5).

The next step is to perform the transformation (6) to the action-angle variables, which are now the fields $I(t,\boldsymbol{x})$ and $\theta(t,\boldsymbol{x})$. The classical action takes the form

$$\begin{aligned}\mathcal{S} &= \int d^4x[\pi_\varphi\partial_t\varphi - \pi_\varphi^2/2 - (\partial_i\varphi)^2/2 - V(\varphi)]\\ &= \int dtd^3\boldsymbol{x}[I\partial_t\theta - \mu I - (\partial_i\varphi)^2/2 - \delta V].\end{aligned} \tag{14}$$

As before, we average the perturbations—the two last terms in Eq. (14)—over period. Expression for $\langle\delta V\rangle$ is already given in Eq. (9). To process the term with spatial derivatives, we substitute Eq. (6) into $(\partial_i\varphi)^2$, move slowly varying $\partial_i I$ and $\partial_i\theta$ out of the average, and then integrate the coefficients in front of them over θ, cf. Eq. (9). This gives

$$\langle(\partial_i\varphi)^2\rangle = \frac{(\partial_i I)^2}{4I\mu} + \frac{I}{\mu}(\partial_i\theta)^2, \tag{15}$$

where the cross-term $\partial_i I\partial_i\theta$ vanishes due to time-reflection symmetry $\theta \to -\theta$.

Substituting Eqs. (9) and (15) into Eq. (14), we arrive at the leading-order effective action for oscillons,[6]

$$\mathcal{S}_{\text{eff}} = \int dtd^3\boldsymbol{x}\left[I\partial_t\theta - \mu I - \frac{(\partial_i I)^2}{8I\mu} - \frac{I(\partial_i\theta)^2}{2\mu} - \frac{\mathcal{A}_p(\varsigma)}{2p} + \frac{\mu I}{2}\right], \tag{16}$$

where $\varsigma = 2I/\mu$ and the function $\mathcal{A}_p(\varsigma)$ is defined in Eq. (10).

The final—important—step is to make the "effective mass" $\mu = \mu(I)$ and its "scale" $\varphi_0 = \varphi_0(I)$ depend on the oscillation amplitude[7] via Eqs. (5) and (11). Like in Sec. II, this tunes μ to the second derivative of the potential at any I.

One can see straight away that the effective model (16) is invariant under the global phase shifts $\theta \to \theta + \alpha$. This implies conservation of the global charge,

$$N = \int d^3\boldsymbol{x}\, I(t,\boldsymbol{x}), \tag{17}$$

representing the adiabatic invariant of Refs. [41,42].

From the viewpoint of the effective theory, oscillons are nontopological solitons [45,46] minimizing the energy E at a fixed charge N. Their profiles can be obtained by extremizing the functional $F = E - \omega N$ with Lagrange multiplier ω, or simply by substituting the stationary ansatz

$$I(t,\boldsymbol{x}) = \psi^2(\boldsymbol{x}), \qquad \theta(t,\boldsymbol{x}) = \omega t, \tag{18}$$

into the effective field equations. Either way, the resulting equation for $\psi(\boldsymbol{x})$ is

$$\begin{aligned}\omega\psi = \mu\psi - \frac{\Delta\psi}{2\mu} + \psi(\partial_i\psi)^2\frac{\partial_I\mu}{2\mu^2}\\ + (\partial_\varsigma\mathcal{A}_p/\mu^2 p - 1/2)(\mu - \psi^2\partial_I\mu)\psi,\end{aligned} \tag{19}$$

cf. Eq. (12) and recall that $\mu = \mu(I)$ is different from the "bare" field mass $m = 1$.

We solve Eq. (19) in spherical symmetry using the shooting method. Figure 3 shows the solutions $\psi = \psi(r)$ at two values of ω. They characterize the oscillon amplitudes which are large and rapidly grow as the frequency ω decreases.

IV. COMPARISON WITH NUMERICAL SIMULATIONS

Let us compare the predictions of our effective field theory (EFT) with exact oscillons. We obtain the latter by numerically evolving the full equation (13) for the spherically symmetric field $\varphi(t,r)$. We start these simulations from the EFT oscillons, i.e., $\varphi(0,r)$ given by the profiles $\psi(r)$ and Eqs. (18), (6). Practice shows that such initial data settle down to true nonexcited oscillons much quicker than generic initial conditions. Details of our numerical method are presented in Ref. [28].

Typical evolution of the oscillon field during one period is visualized in Fig. 4, where solid and dashed lines correspond to oscillation maximum and minimum, respectively. In the

[6] One may pack real I and θ into one complex field $\psi(t,\boldsymbol{x}) = \sqrt{I}\mathrm{e}^{-i\theta}$; see Ref. [28]. This turns the effective theory (16) into a nonlinear Schrödinger model with global symmetry $\psi \to \psi\mathrm{e}^{-i\alpha}$.

[7] One can show that the effective action (16) is insensitive to φ_0 up to $O(\varepsilon^2)$ corrections, where $\delta V \sim (\partial_i I)^2/I \sim O(\varepsilon)$.

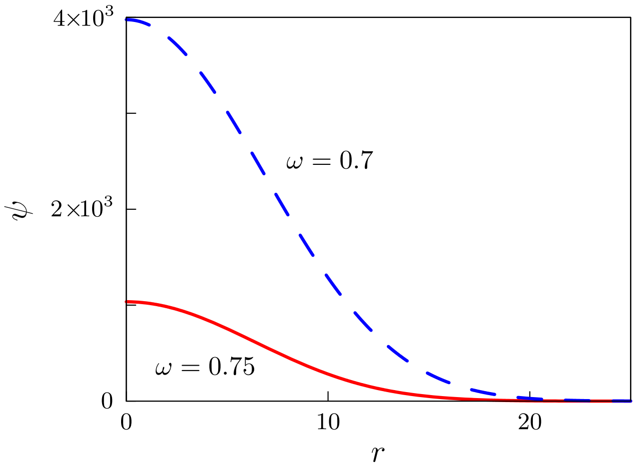

FIG. 3. Profiles $\psi(r)$ of the monodromy oscillons at two frequencies and $p = 0.95$.

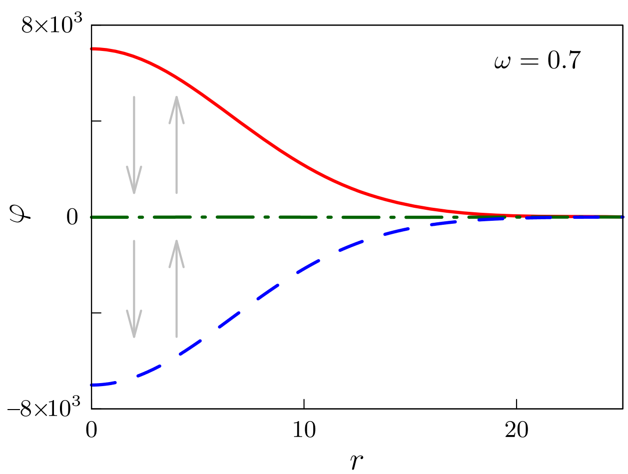

FIG. 4. Numerical evolution of the monodromy oscillon during one period. We use $\omega = 0.7$ and $p = 0.95$.

exact model, outgoing radiation carries away the energy and makes the oscillon amplitude decrease, but that process is extremely slow and cannot be seen in Fig. 4.

Once the exact oscillon is formed, we measure its period $T = 2\pi/\omega$ as the time interval between the consecutive maxima of the field at the center $\varphi(t, 0)$. The "exact" value of the adiabatic invariant N is given by the standard formula [41,42],

$$N = \frac{1}{2\pi}\int d^3\boldsymbol{x} \oint \pi_\varphi d\varphi = \int d^3\boldsymbol{x} \int_t^{t+T} \frac{dt}{2\pi}(\partial_t\varphi)^2. \quad (20)$$

Finally, the oscillon energy E is

$$E = \int d^3\boldsymbol{x}[(\partial_t\varphi)^2/2 + (\partial_i\varphi)^2/2 + V(\varphi)]. \quad (21)$$

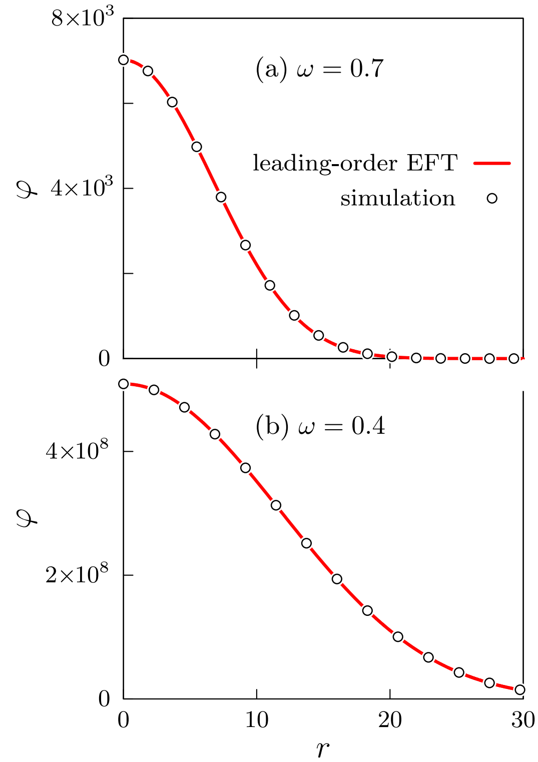

FIG. 5. Fields $\varphi(t_{\max}, r)$ of the monodromy oscillons at times $t_{\max}$ of oscillation maxima. We use $p = 0.95$ and frequencies (a) $\omega = 0.7$, (b) $\omega = 0.4$. Solid line is the EFT prediction, while the circles show results of full numerical simulations.

To increase precision, we average all "exact" quantities over several periods.

In Fig. 5 we compare the fields $\varphi(t, \boldsymbol{x})$ of numerical and EFT oscillons with the same frequency ω at the moments $t_{\max}$ of oscillation maxima, $\partial_t\varphi(t_{\max}, 0) = 0$. The EFT prediction (lines) is obtained by substituting the profile $I = \psi^2(r)$ into Eq. (6) at $\theta = 0$. It agrees well with the numerical results (circles) at two essentially different values of ω. Note that our theory remains precise even for the $\omega = 0.4$ oscillon that has extremely large amplitude. We further confirm this in Fig. 6(a) showing the maximal fields $\varphi(t_{\max}, r = 0)$ of exact and EFT oscillons as functions of frequency.

Good agreement is also observed for the integral quantities, say, the oscillon charge[8] $N(\omega)$ given by Eq. (17) in the EFT and by Eq. (20) in full theory, cf. the lines and circles in Fig. 6(b). It is worth noting that oscillons with $\omega \lesssim 0.99$ satisfy the Vakhitov-Kolokolov criterion [28,47,48] $dN/d\omega < 0$ which is necessary for stability. Thus, they are expected to be unstable with respect to linear perturbations only in the narrow frequency region $\omega \approx m = 1$.

[8]Graphs for $E(\omega)$ and $N(\omega)$ have similar shapes due to the relation $dE/dN = \omega$ holding for the EFT oscillons [28].

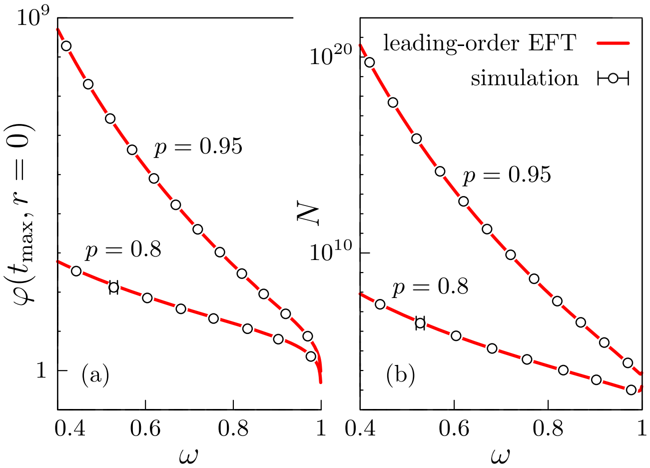

FIG. 6. (a) Amplitudes $\varphi(t_{\max}, r=0)$ and (b) adiabatic invariants $N(\omega)$ of the monodromy oscillons at $p = 0.8$ and $p = 0.95$. Solid lines show the predictions of the leading-order EFT. At two values of p, they reproduce the exact numerical results (circles) with relative precisions $\Delta N/N \sim 0.2$ and 0.06, respectively. The latter accuracies are almost independent of the oscillon amplitude.

To sum up, our leading-order EFT with field-dependent "mass" $\mu = \mu(I)$ gives accurate predictions even if the monodromy potential is moderately nonlinear; see the graph with $p = 0.8$ and $\varepsilon = 0.2$ in Fig. 6. Their relative error is almost insensitive to the field strength inside the oscillon but grows with nonlinearity of the potential.

V. HIGHER-ORDER CORRECTIONS

So far, we used the leading-order approximation: We assumed that I and θ evolve slowly while evaluating the averages $\delta V \to \langle \delta V \rangle$ in Eq. (9) and $(\partial_i \varphi)^2 \to \langle (\partial_i \varphi)^2 \rangle$ in Eq. (15). Let us show that this approach can be promoted to a consistent asymptotic expansion in the nonlinearity δV of the potential and in the inverse oscillon size R^{-1}.

We split I and θ into EFT fields $\bar{I}$, $\bar{\theta}$ evolving at large timescales and fast-oscillating corrections δI, $\delta\theta$,

$$I = \bar{I}(t, \boldsymbol{x}) + \delta I(t, \boldsymbol{x}), \qquad \theta = \bar{\theta}(t, \boldsymbol{x}) + \delta\theta(t, \boldsymbol{x}), \tag{22}$$

where $\langle \delta I \rangle = \langle \delta\theta \rangle = 0$. Effective action for $\bar{I}$ and $\bar{\theta}$ can be computed by integrating out δI and $\delta\theta$ in the arbitrary slowly changing background. To this end, we obtain exact equations for I and θ from the action (14) and subtract their time averages. We get

$$\partial_t \delta I = j_\theta(I, \theta), \qquad \partial_t \delta\theta = -j_I(I, \theta), \tag{23}$$

where

$$j_\theta = \partial_\theta \varphi (\Delta\varphi - \delta V'), \tag{24}$$

$$j_I = \partial_I \varphi (\Delta\varphi - \delta V') - \langle \partial_I \varphi (\Delta\varphi - \delta V') \rangle \tag{25}$$

are the sources depending on $\bar{I}$, $\bar{\theta}$, δI, and $\delta\theta$ via Eqs. (6) and (22).

It is clear that Eqs. (23) can be used to express δI and $\delta\theta$ as functions of $\bar{I}$ and $\bar{\theta}$. Indeed, let us change the time variable to $\bar{\theta}$ which evolves progressively: $\partial_t \approx (\partial_t \bar{\theta}) \partial_{\bar{\theta}}$. Then, solving the equations order-by-order in small δI and $\delta\theta$, we indeed find the fast-oscillating parts as series of functions depending on $\bar{I}$ and $\bar{\theta}$.

Let calculate the first nontrivial (second-order) correction to the effective action considering the stationary oscillon background $\bar{I} = \psi^2(\boldsymbol{x})$ and $\bar{\theta} = \omega t$ in Eq. (18). At this level, we ignore δI and $\delta\theta$ in the right-hand sides of Eqs. (23). Then

$$j_\theta \approx \frac{\sin 2\bar{\theta}}{\mu} \psi^2 [-\Delta\psi/\psi - \mu^2 + (1 + \varsigma \cos^2 \bar{\theta})^{-\varepsilon}], \tag{26}$$

$$j_I \approx \frac{\cos 2\bar{\theta}}{2\mu} \left(\frac{\Delta\psi}{\psi} + \mu^2 \right) - \frac{\cos^2 \bar{\theta}}{\mu} (1 + \varsigma \cos^2 \bar{\theta})^{-\varepsilon} + \frac{1}{2\psi^2} [\mathcal{A}_p(\varsigma) - \mathcal{A}_{p-1}(\varsigma)], \tag{27}$$

where Eqs. (6), the monodromy potential (1), (2), and $\varsigma = 2\bar{I}/\mu$ were used. The solutions $\delta I(\bar{I}, \bar{\theta})$ and $\delta\theta(\bar{I}, \bar{\theta})$ are given by the primitives of the sources (26), (27), with respect to $\bar{\theta}$. We substitute them into the action (14) expanded quadratically in δI and $\delta\theta$ and average the result over $\bar{\theta}$. This gives the second-order effective action $\mathcal{S}_{\text{eff}} = \mathcal{S}_{\text{eff}}^{(1)} + \mathcal{S}_{\text{eff}}^{(2)}$, where $\mathcal{S}_{\text{eff}}^{(1)}[\bar{I}, \bar{\theta}]$ is provided by Eq. (16) and the correction is

$$\begin{aligned} \mathcal{S}_{\text{eff}}^{(2)} &= \frac{1}{\omega} \int dt d^3\boldsymbol{x} \left\langle j_I(\bar{I}, \bar{\theta}) \int^{\bar{\theta}} j_\theta(\bar{I}, \bar{\theta}') d\bar{\theta}' \right\rangle \\ &= \frac{1}{4\omega} \int dt d^3\boldsymbol{x} \left\{ \frac{1}{2\mu^2} (\Delta\psi + \mu^2 \psi)^2 + \frac{\mathcal{D}_p(\varsigma)}{p\psi^2} - \frac{\mathcal{B}_p(\varsigma)}{p\psi^3} (\Delta\psi + \mu^2\psi) \right\}; \end{aligned} \tag{28}$$

see Ref. [28] for general and detailed discussion. In Eq. (28) we introduced the form factors

$$\mathcal{B}_p = (p+1)\mathcal{A}_{p+1}(\varsigma) + p(\varsigma/2 + 1)\mathcal{A}_{p-1}(\varsigma) - (1 + 2p + (p+1)\varsigma/2)\mathcal{A}_p(\varsigma), \tag{29}$$

$$\mathcal{D}_p = \mathcal{A}_{2p}(\varsigma) - \mathcal{A}_p^2(\varsigma) - \mathcal{A}_{2p-1}(\varsigma) + \mathcal{A}_p(\varsigma)\mathcal{A}_{p-1}(\varsigma) \tag{30}$$

in front of the terms with different numbers of derivatives.

The second-order effective theory remains invariant under the shifts $\bar{\theta} \to \bar{\theta} + \alpha$ due to averaging over $\bar{\theta}$. This means that the global charge N is still conserved. Its Noether expression

$$N = \int d^3\boldsymbol{x}\, \frac{\delta \mathcal{S}_{\text{eff}}}{\delta \partial_t \bar{\theta}},$$

however, includes a correction to Eq. (17) because $\mathcal{S}_{\text{eff}}^{(2)}$ depends on $\partial_t \bar{\theta} = \omega$.

After finding $\mathcal{S}_{\text{eff}}^{(2)}$, we again allow φ_0 and μ to vary with $I \to \bar{I}$ via Eqs. (11) and (5). This time, the effective action is sensitive to φ_0 at the weaker level $O(\varepsilon^3)$.

The action (16), (28) allows us to compute corrections to the oscillon profiles $\psi(r) = \psi^{(1)}(r) + \psi^{(2)}(r)$, their fields $\varphi(\bar{I} + \delta I, \bar{\theta} + \delta\theta)$, charges, and energies.

Let us juxtapose the improved theory with exact simulations. However, we saw that the accuracy of our leading-order EFT is already comparable to the numerical precision. To see the progress, we intentionally spoil the theory by choosing a counterintuitive auxiliary scale $\varphi_0^2 = \bar{I}/128 \ll \bar{I}$, cf. Eq. (6). Besides, we use essentially nonquadratic potential with $p = 0.8$ and $\varepsilon = 0.2$. Together, these deteriorations move the leading-order predictions for $N(\omega)$ away from the exact result, cf. the dashed line with the circles in Fig. 7. But the second-order EFT (solid line) is less susceptible to the impairment and agrees with the simulations. This demonstrates that higher-order corrections are capable of improving the effective theory, although they are impractical in the model under consideration.

It is worth noting that corrections to the effective action of even higher orders can be computed similarly to Eq. (28), in two steps. First, solve Eqs. (23) to the required order in δI and $\delta\theta$ and substitute the result into the action (14) expanded to the same order. Second, average the resulting Lagrangian over $\bar{\theta}$. The possibility of performing calculations to arbitrary order exposes our effective theory as asymptotic expansion and clarifies its region of applicability.

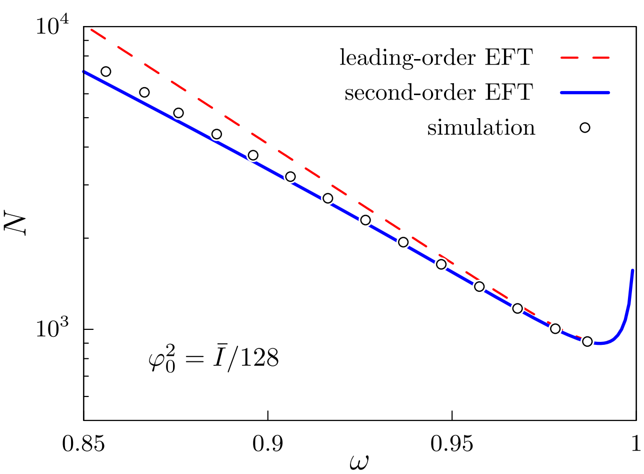

FIG. 7. Comparison of the first- and second-order EFT predictions (lines) with exact simulations (circles). The plot shows the charge $N(\omega)$ of the monodromy oscillons at $p = 0.8$. We intentionally ruined the precision of the theoretical calculation by detuning the parameter φ_0.

VI. DISCUSSION

We developed a simple and precise analytic description of oscillons in scalar models with nearly quadratic potentials. The two cornerstones of our method are the correct choice of variables I, θ in Eq. (6) and the "running" (field-dependent) mass $\mu(I)$ in Eqs. (2), (5), and (11). We demonstrated that the effective action (16), (28) for I and θ has the form of a systematic asymptotic expansion in the spatial derivatives and nonlinearities of the potential. Oscillons appear in this effective theory as nontopological solitons minimizing the energy at a given value of the adiabatic invariant N.

The best part of our method is the possibility of computing corrections by keeping more terms in the expansion. At the same time, suitable choice of the "running mass" μ radically improves precision, making credible even the leading-order results. This trick with μ is inspired by the renormalization theory: it does the same job for the effective classical action as scale-dependent coupling constants do for the perturbative QFT. We demonstrate its power once again in Fig. 8 by plotting the energy $E(\omega)$ of oscillons in the monodromy model (1) as a function of their frequency ω at $p = 0.95$. Relative deviation of our leading-order theoretical prediction (solid line) from the exact simulation (circles) never exceeds $\Delta E/E \lesssim 0.06$ despite the fact that fields inside the oscillons are exceptionally strong at small ω.

It is instructive to compare our new theory with other analytic approaches. In the perturbative (small-amplitude) method, one expands the monodromy potential (1) in powers of φ,

$$V = \varphi^2/2 - \varepsilon\varphi^4/4 + \varepsilon(1+\varepsilon)\varphi^6/12 + \ldots \tag{31}$$

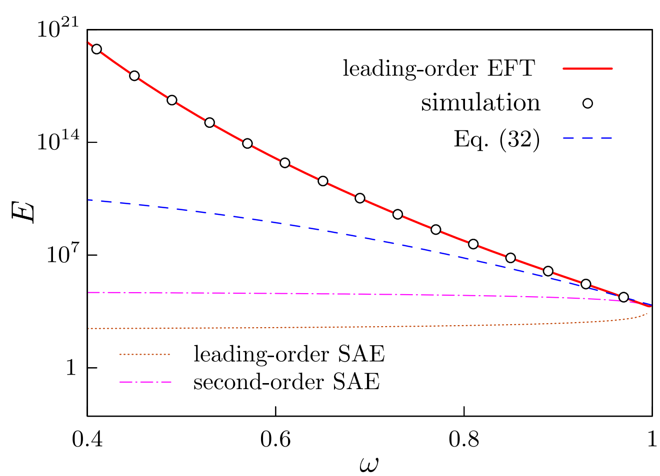

FIG. 8. The energy $E(\omega)$ of three-dimensional monodromy oscillons at $p = 0.95$ and $\varepsilon = 0.05$.

and then solves the field equation order-by-order in it [35–39]. Generally speaking, such small-amplitude expansion (SAE) is valid only at $\omega \sim m = 1$, since it can be recast as series in the binding energy $(1-\omega) \propto \varphi^2$ of particles inside the oscillons [35]. This is apparent in Fig. 8, where the dotted and dash-dotted lines show the first two orders of SAE [two and three terms in Eq. (31), respectively]. In the most interesting and wide frequency region $\omega \lesssim 0.9$ they considerably deviate from the simulations.

Another method employs expansion in $\varepsilon \equiv 1-p$ characterizing nonlinearity of the monodromy potential (1). At the first order and $|\varphi| \gg 1$ one obtains [9],

$$V = \frac{\varphi^2}{2}[1+\varepsilon - \varepsilon \ln \varphi^2 + O(\varphi^{-2}) + O(\varepsilon^2 \ln^2|\varphi|)]. \qquad (32)$$

This truncated model has a family of exactly periodic solutions with Gaussian spatial profiles [9,42,49] that approximate the monodromy oscillons—see the dashed line in Fig. 8 showing their energies. We observe that Eq. (32) does a better job than the small-amplitude expansion, but fails at small ω when oscillon fields become exceptionally large, $\varepsilon \ln|\varphi| \gtrsim 1$.

In contrast, our effective theory universally applies and remains precise at all frequencies and oscillon amplitudes. Its relative accuracy is rather controlled by the anharmonicity parameter $\varepsilon \equiv 1-p$ of the potential. For example, in the model of monodromy inflation [12–15] with $p = 0.5$ the leading-order EFT results for the oscillon energies are offset by $\Delta E/E \sim 0.4$ from the exact data, cf. the dashed line and the circles in Fig. 9. However, one can make a better choice of the EFT parameter φ_0: find it by solving the equation $\varphi_0^2 = 2I/\mu(\varphi_0)$. Then the relative error drops down to $\Delta E/E \sim 0.1$ which is surprisingly small; see the solid line in Fig. 9 and Footnote 5 for details. This suggests that the wise choice of the EFT scale is capable of curing the method even in the case of significantly nonlinear potentials.[9]

We anticipate that the results of this paper will be helpful for analytic calculations in oscillon cosmology. In particular, theoretical relations between oscillon amplitudes, energies, frequencies, and adiabatic charges are important whenever these objects represent dark matter [9,25] or generate gravitational waves after inflation [16,27,29]. Even more results can be obtained by applying our method in other models with nearly quadratic potentials akin to Eq. (1).

[9]This does not mean, however, that the EFT series converge well in this case, since the expansion parameter $\varepsilon = 0.5$ is large.

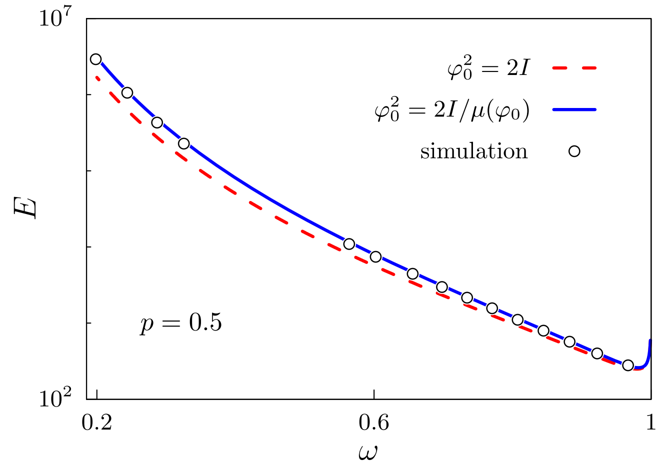

FIG. 9. Oscillon energies $E(\omega)$ in the case of strongly nonlinear monodromy potential with $p = 0.5$ (points) compared to the two leading-order EFT predictions (solid and dashed lines). The latter lines differ by the choice of the EFT scale φ_0.

But the most interesting development would be to adopt our approach for calculation of the oscillon evaporation rates Γ. Segur and Kruskal evaluated them analytically in the framework of small-amplitude expansion [37]; see also [39,50,51]. Namely, they demonstrated that $\Gamma \propto \exp(-\mathrm{const}/g_0)$ is nonperturbative in the expansion parameter $g_0 \propto \varphi$. Our technique is different, but it also has the form of asymptotic expansion. Its formal parameter g can be introduced in Eq. (2) as

$$V = \mu^2 \varphi^2/2 + g^2 \delta V,$$

where $g = 1$ is the physical value. Once this is done, the rescaling $\boldsymbol{x} = \tilde{\boldsymbol{x}}/g$ brings g^2 in front of the second small term with spatial derivatives. It would be fascinating to apply methods of nonperturbative resummation in Refs. [37,39,50,51] to our series, thus getting a general expression for Γ in models with nearly quadratic potentials. The latter calculation, however, lies beyond the scope of the present paper.

ACKNOWLEDGMENTS

We thank E. Nugaev and A. Panin for fierce discussions. This work was supported by the RSF Grant No. 22-12-00215. Numerical calculations were performed on the Computational Cluster of the Theoretical Division of INR RAS.

[1] A. E. Kudryavtsev, Solitonlike solutions for a Higgs scalar field, JETP Lett. **22**, 82 (1975), http://jetpletters.ru/ps/1522/article_23290.shtml.

[2] I. L. Bogolyubsky and V. G. Makhankov, On the pulsed soliton lifetime in two classical relativistic theory models, JETP Lett. **24**, 12 (1976), http://jetpletters.ru/ps/1809/article_27642.shtml.

[3] M. Gleiser, Pseudostable bubbles, Phys. Rev. D **49**, 2978 (1994).

[4] E. W. Kolb and I. I. Tkachev, Nonlinear axion dynamics and formation of cosmological pseudosolitons, Phys. Rev. D **49**, 5040 (1994).

[5] P. Salmi and M. Hindmarsh, Radiation and relaxation of oscillons, Phys. Rev. D **85**, 085033 (2012).

[6] M. A. Amin, K-oscillons: Oscillons with noncanonical kinetic terms, Phys. Rev. D **87**, 123505 (2013).

[7] J. Sakstein and M. Trodden, Oscillons in higher-derivative effective field theories, Phys. Rev. D **98**, 123512 (2018).

[8] P. Dorey, T. Romanczukiewicz, and Y. Shnir, Staccato radiation from the decay of large amplitude oscillons, Phys. Lett. B **806**, 135497 (2020).

[9] J. Olle, O. Pujolas, and F. Rompineve, Recipes for oscillon longevity, J. Cosmol. Astropart. Phys. 09 (2021) 015.

[10] T. S. Mendonça and H. P. de Oliveira, Quest for eternal oscillons, Phys. Rev. D **105**, 116028 (2022).

[11] F. van Dissel, O. Pujolas, and E. Sfakianakis, Oscillon spectroscopy, J. High Energy Phys. 07 (2023) 194.

[12] K. D. Lozanov and M. A. Amin, End of inflation, oscillons, and matter-antimatter asymmetry, Phys. Rev. D **90**, 083528 (2014).

[13] J. Liu, Z.-K. Guo, R.-G. Cai, and G. Shiu, Gravitational Waves from Oscillons with Cuspy Potentials, Phys. Rev. Lett. **120**, 031301 (2018).

[14] E. Cotner, A. Kusenko, M. Sasaki, and V. Takhistov, Analytic description of primordial black hole formation from scalar field fragmentation, J. Cosmol. Astropart. Phys. 10 (2019) 077.

[15] K. D. Lozanov, M. Sasaki, and V. Takhistov, Universal gravitational wave signatures of cosmological solitons, arXiv:2304.06709.

[16] M. A. Amin, R. Easther, H. Finkel, R. Flauger, and M. P. Hertzberg, Oscillons After Inflation, Phys. Rev. Lett. **108**, 241302 (2012).

[17] J.-P. Hong, M. Kawasaki, and M. Yamazaki, Oscillons from pure natural inflation, Phys. Rev. D **98**, 043531 (2018).

[18] R. Mahbub and S. S. Mishra, Oscillon formation from preheating in asymmetric inflationary potentials, arXiv:2303.07503.

[19] J. C. Aurrekoetxea, K. Clough, and F. Muia, Oscillon formation during inflationary preheating with general relativity, Phys. Rev. D **108**, 023501 (2023).

[20] E. J. Copeland, M. Gleiser, and H. R. Muller, Oscillons: Resonant configurations during bubble collapse, Phys. Rev. D **52**, 1920 (1995).

[21] I. Dymnikova, L. Koziel, M. Khlopov, and S. Rubin, Quasilumps from first order phase transitions, Gravitation Cosmol. **6**, 311 (2000).

[22] M. Gleiser, N. Graham, and N. Stamatopoulos, Long-lived time-dependent remnants during cosmological symmetry breaking: From inflation to the electroweak scale, Phys. Rev. D **82**, 043517 (2010).

[23] A. Vaquero, J. Redondo, and J. Stadler, Early seeds of axion miniclusters, J. Cosmol. Astropart. Phys. 04 (2019) 012.

[24] M. Buschmann, J. W. Foster, and B. R. Safdi, Early Universe Simulations of the Cosmological Axion, Phys. Rev. Lett. **124**, 161103 (2020).

[25] J. Ollé, O. Pujolàs, and F. Rompineve, Oscillons and dark matter, J. Cosmol. Astropart. Phys. 02 (2020) 006.

[26] D. Cyncynates and T. Giurgica-Tiron, Structure of the oscillon: The dynamics of attractive self-interaction, Phys. Rev. D **103**, 116011 (2021).

[27] Y. Sang and Q.-G. Huang, Stochastic gravitational-wave background from axion-monodromy oscillons in string theory during preheating, Phys. Rev. D **100**, 063516 (2019).

[28] D. G. Levkov, V. E. Maslov, E. Y. Nugaev, and A. G. Panin, An effective field theory for large oscillons, J. High Energy Phys. 12 (2022) 079.

[29] S.-Y. Zhou, E. J. Copeland, R. Easther, H. Finkel, Z.-G. Mou, and P. M. Saffin, Gravitational waves from oscillon preheating, J. High Energy Phys. 10 (2013) 026.

[30] E. Silverstein and A. Westphal, Monodromy in the CMB: Gravity waves and string inflation, Phys. Rev. D **78**, 106003 (2008).

[31] L. McAllister, E. Silverstein, and A. Westphal, Gravity waves and linear inflation from axion monodromy, Phys. Rev. D **82**, 046003 (2010).

[32] M. Cicoli, J. P. Conlon, A. Maharana, S. Parameswaran, F. Quevedo, and I. Zavala, String cosmology: From the early universe to today, arXiv:2303.04819.

[33] M. A. Amin and D. Shirokoff, Flat-top oscillons in an expanding universe, Phys. Rev. D **81**, 085045 (2010).

[34] N. S. Manton and T. Romańczukiewicz, Simplest oscillon and its sphaleron, Phys. Rev. D **107**, 085012 (2023).

[35] A. Kosevich and A. Kovalev, Self-localization of vibrations in a one-dimensional anharmonic chain, Sov. Phys. JETP **40**, 891 (1975), http://jetp.ras.ru/cgi-bin/e/index/e/40/5/p891?a=list.

[36] R. F. Dashen, B. Hasslacher, and A. Neveu, The particle spectrum in model field theories from semiclassical functional integral techniques, Phys. Rev. D **11**, 3424 (1975).

[37] H. Segur and M. D. Kruskal, Nonexistence of Small-Amplitude Breather Solutions in ϕ^4 Theory, Phys. Rev. Lett. **58**, 747 (1987).

[38] G. Fodor, P. Forgacs, Z. Horvath, and A. Lukacs, Small amplitude quasi-breathers and oscillons, Phys. Rev. D **78**, 025003 (2008).

[39] G. Fodor, A review on radiation of oscillons and oscillatons, Ph.D. thesis, Wigner RCP, Budapest, 2019, arXiv:1911.03340.

[40] M. Gleiser, d-Dimensional oscillating scalar field lumps and the dimensionality of space, Phys. Lett. B **600**, 126 (2004).

[41] S. Kasuya, M. Kawasaki, and F. Takahashi, I-balls, Phys. Lett. B **559**, 99 (2003).

[42] M. Kawasaki, F. Takahashi, and N. Takeda, Adiabatic invariance of oscillons/I-balls, Phys. Rev. D **92**, 105024 (2015).

[43] H.-Y. Zhang, M. A. Amin, E. J. Copeland, P. M. Saffin, and K. D. Lozanov, Classical decay rates of oscillons, J. Cosmol. Astropart. Phys. 07 (2020) 055.

[44] J. Eby, P. Suranyi, C. Vaz, and L. C. R. Wijewardhana, Axion Stars in the Infrared Limit, J. High Energy Phys. 03 (2015) 080; 11 (2016) 134(E).

[45] S. R. Coleman, Q-balls, Nucl. Phys. **B262**, 263 (1985); **B269**, 744(E) (1986).

[46] E. Y. Nugaev and A. V. Shkerin, Review of nontopological solitons in theories with $U(1)$-symmetry, J. Exp. Theor. Phys. **130**, 301 (2020).

[47] N. G. Vakhitov and A. A. Kolokolov, Stationary solutions of the wave equation in a medium with nonlinearity saturation, Radiophys. Quantum Electron. **16**, 783 (1973).

[48] V. E. Zakharov and E. A. Kuznetsov, Solitons and collapses: Two evolution scenarios of nonlinear wave systems, Phys. Usp. **55**, 535 (2012).

[49] G. Dvali and A. Vilenkin, Solitonic D-branes and brane annihilation, Phys. Rev. D **67**, 046002 (2003).

[50] G. Fodor, P. Forgacs, Z. Horvath, and M. Mezei, Computation of the radiation amplitude of oscillons, Phys. Rev. D **79**, 065002 (2009).

[51] G. Fodor, P. Forgacs, Z. Horvath, and M. Mezei, Radiation of scalar oscillons in 2 and 3 dimensions, Phys. Lett. B **674**, 319 (2009).